A Simple Stochastic Dynamical Model Capturing the Statistical Diversity of El Niño Southern Oscillation

Nan Chen[1] and Andrew J. Majda[1,2]

Corresponding author: Nan Chen, Department of Mathematics and Center for Atmosphere Ocean Science, Courant Institute of Mathematical Sciences, New York University, 251 Mercer Street, New York, NY 10012, USA. (chennan@cims.nyu.edu)

[1]Department of Mathematics and Center for Atmosphere Ocean Science, Courant Institute of Mathematical Sciences, New York University, 251 Mercer Street, New York, NY 10012, USA.

[2]Center for Prototype Climate Modeling, New York University Abu Dhabi, Saadiyat Island, Abu Dhabi, UAE.

Key Points.

- A stochastic state-dependent wind bursts process including both westerly and easterly wind is coupled to a simple ocean-atmosphere model
- Nonlinear zonal advection, mean easterly trade wind anomaly and effective stochastic noise facilitate the occurrence of the CP El Nino
- Non-Gaussian statistical properties in different Nino regions are captured and all types of ENSO events are produced with realistic features

Abstract

The El Niño Southern Oscillation (ENSO) has significant impact on global climate and seasonal prediction. A simple modeling framework is developed here that automatically captures the statistical diversity of ENSO. First, a stochastic parameterization of the wind bursts including both westerly and easterly wind is coupled to a simple ocean-atmosphere model that is otherwise deterministic, linear and stable. Then a simple nonlinear zonal advection and a mean easterly trade wind anomaly are incorporated into the coupled system that enables anomalous warm sea surface temperature in the central Pacific. The state-dependent wind activity is driven by a three-state Markov jump process, which allows the coupled model to simulate the traditional moderate El Niño, the super El Niño, the central Pacific El Niño and the La Niña with realistic features. The corresponding Walker circulation anomalies resemble those in nature. Importantly, the model captures the non-Gaussian statistical characteristics in different Nino regions.

1. Introduction

The El Niño Southern Oscillation (ENSO) is the most prominent interannual climate variability on earth with large ecological and societal impacts. It consists of a cycle of anomalously warm El Niño conditions and cold La Niña conditions with considerable irregularity in amplitude, duration, temporal evolution and spatial structure. The traditional El Niño involves anomalous warm sea surface temperature (SST) in the equatorial eastern Pacific ocean, where its atmospheric response is the eastward shift of the anomalous Walker circulation [*Clarke*, 2008].

While the difference among traditional ENSO events have been known for many years, a renewed interest in the ENSO diversity is stimulated by a different type of El Niño that is frequently observed in recent decades and is called the central Pacific (CP) El Niño [*Lee and McPhaden*, 2010; *Kao and Yu*, 2009; *Ashok et al.*, 2007; *Kug et al.*, 2009; *Larkin and Harrison*, 2005; *Guilyardi*, 2006]. The CP El Niño is characterized by warm SST anomalies confined to the central Pacific, flanked by colder waters to both east and west. Such zonal SST gradients result in an anomalous two-cell Walker circulation over the tropical Pacific, with a strong convection locating in the central Pacific. Different from the traditional El Niño which is strongly associated with thermocline variations, the CP El Niño appears more related to zonal advection and atmospheric forcing [*Kao and Yu*, 2009; *Yu and Kao*, 2007; *Yeh et al.*, 2009, 2014; *Ren and Jin*, 2013]. Particularly, accompanying with the increasing occurrence of the CP El Niño since 1990's, a recent multidecadal acceleration of easterly trade winds is observed [*England et al.*, 2014; *Sohn et al.*, 2013; *Merrifield and Maltrud*, 2011] which is linked with the strengthening of the Walker circulation [*L'Heureux* *et al.*, 2013; *Choi et al.*, 2016; *McGregor et al.*, 2014]. In addition to the distinct climate patterns in the equatorial Pacific region, the ENSO diversity also has strong impact on global climate and seasonal prediction through teleconnections [*Ashok et al.*, 2007; *Weng et al.*, 2009], and is suggested as a possible link with climate change [*Capotondi et al.*, 2015].

Despite the significant impact of ENSO, current climate models have biases in simulating the ENSO diversity. In fact, most of the general circulation models (GCMs) are able to reproduce only one single type of El Niño and the simulated ENSO variability is usually sensitive to parameter perturbations [*Ham and Kug*, 2012; *Kug et al.*, 2012; *Ault et al.*, 2013]. Other climate models can reproduce the observed diversity of ENSO to some extent [*Kim and Yu*, 2012; *Yu and Kim*, 2010]. However, the amplitudes of the ENSO interannual variability is generally overestimated and the frequency and duration of the ENSO events differ from nature [*Wittenberg*, 2009; *Kug et al.*, 2010]. In addition, the moderate CP El Niño events simulated by some GCMs are located farther west than the real observations [*Capotondi et al.*, 2015]. Therefore, designing simple dynamical models including the ENSO diversity is crucial in both understanding nature and providing guidelines to improve the GCMs.

In this article, a simple modeling framework is developed that automatically captures key features and the statistical diversity of ENSO. The starting model involves a coupled ocean-atmosphere model that is deterministic, linear and stable. Then systematic strategies are developed for incorporating several major causes of the ENSO diversity into the coupled system. First, due to the fact that atmospheric wind bursts play a key role in triggering the ENSO events, a stochastic parameterization of the wind bursts including both westerly and easterly wind is coupled to the simple ocean-atmosphere system, where the amplitude of the wind bursts depends on the strength of SST in the western Pacific warm pool. The coupled model succeeds in recovering the traditional El Niño and La Niña and captures key features of the observational record in the eastern Pacific [*Thual et al.*, 2016]. Secondly, a simple nonlinear zonal advection with no ad hoc parameterization of the background SST gradient is introduced that creates a coupled nonlinear advective mode of SST. In addition, due to the recent multidecadal strengthening of the easterly trade wind, a mean easterly trade wind anomaly is incorporated into the stochastic parameterization of the wind activity. The combined effect of the nonlinear zonal advection, the enhanced mean easterly trade wind anomaly and the effective stochastic noise facilitates the intermittent occurrence of the CP El Niño [*Chen and Majda*, 2016]. Finally, a three-state Markov jump process is developed to drive the stochastic wind activity, which allows the coupled model to simulate different types of ENSO events with realistic features.

The subsequent sections present the coupled ocean-atmosphere system, the stochastic wind burst model and the Markov jump process as well as the statistical diversity of ENSO simulated by the coupled model. Details of model derivations, choice of parameters and sensitivity tests are included in the Supporting Information.

2. Coupled ENSO model

2.1. ENSO model

The ENSO model consists of a non-dissipative atmosphere coupled to a simple shallow-water ocean and SST budget [*Thual et al.*, 2016; *Chen and Majda*, 2016]:

Interannual atmosphere model

$$\begin{aligned}&-yv - \partial_x\theta = 0\\&yu - \partial_y\theta = 0\\&-(\partial_x u + \partial_y v) = E_q/(1-\overline{Q}),\end{aligned}\tag{1}$$

Interannual ocean model

$$\begin{aligned}&\partial_\tau U - c_1 YV + c_1\partial_x H = c_1\tau_x\\&YU + \partial_Y H = 0\\&\partial_\tau H + c_1(\partial_x U + \partial_Y V) = 0,\end{aligned}\tag{2}$$

Interannual SST model

$$\partial_\tau T + \underline{\mu\partial_x(UT)} = -c_1\zeta E_q + c_1\eta H,\tag{3}$$

with

$$\begin{aligned}&E_q = \alpha_q T\\&\tau_x = \gamma(u+u_p).\end{aligned}\tag{4}$$

In (1)–(4), x is zonal direction and τ is interannual time, while y and Y are meridional direction in the atmosphere and ocean, respectively. The u, v are zonal and meridional winds, θ is potential temperature, U, V, are zonal and meridional currents, H is thermocline depth, T is SST, E_q is latent heating, and τ_x is zonal wind stress. All variables are anomalies from an equilibrium state, and are non-dimensional. The coefficient c_1 is a non-dimensional ratio of time scales, which is of order $O(1)$. The term u_p in (4) describes stochastic wind burst activity (See Section 2.2). The atmosphere extends over the entire equatorial belt $0 \le x \le L_A$ with periodic boundary conditions, while the Pacific ocean extends over $0 \le x \le L_O$ with reflection boundary conditions for the ocean model and zero normal derivative at the boundaries for the SST model.

The above model retains a few essential processes that model the ENSO dynamics in a simple fashion. Latent heating E_q, proportional to SST, is depleted from the ocean and forces an atmospheric circulation. The resulting zonal wind stress τ_x in return forces an ocean circulation that imposes feedback on the SST through thermocline depth anomalies H. This thermocline feedback η is more significant in the eastern Pacific, as shown in Figure 1.

The coupled model introduces unique theoretical elements such as a non-dissipative atmosphere consistent with the skeleton model for the Madden-Julian oscillation (MJO) [*Majda and Stechmann*, 2009, 2011], valid here on the interannual timescale and suitable to describe the dynamics of the Walker circulation [*Majda and Klein*, 2003; *Stechmann and Ogrosky*, 2014; *Stechmann and Majda*, 2015]. In addition, the meridional axis y and Y are different in the atmosphere and ocean as they each scale to a suitable Rossby radius. This allows for a systematic meridional decomposition of the system into the well-known parabolic cylinder functions [*Majda*, 2003], which keeps the system low-dimensional [*Thual et al.*, 2013]. Here, model (1) and (2)–(3) are projected and truncated to the first parabolic cylinder function of the atmosphere [*Majda and Stechmann*, 2009], and the ocean [*Clarke*, 2008], respectively. Details are included in the Supporting Information.

The coupled system (1)–(4) without the nonlinear zonal advection in (3) was systematically studied in [*Thual et al.*, 2016]. It succeeds in recovering the traditional El Niño with occasionally super El Niño and capturing the ENSO statistics in the eastern Pacific as in nature. Note that if the stochastic wind burst u_p is further removed, the resulting coupled system is linear, deterministic and stable.

The observational significance of the zonal advection has been shown for the CP El Niño [*Kug et al.*, 2009; *Su et al.*, 2014]. Different from the previous works [*Jin and An*, 1999; *Dewitte et al.*, 2013] where the advection is mostly linear and requires ad hoc parameterization of the background SST gradient, a simple nonlinear advection is adopted in (3) that contributes significantly to the SST tendency. Such nonlinear advection provides the mechanism of transporting anomalous warm water to the central Pacific region by the westward ocean zonal current. Importantly, when stochasticity is included in the wind activity u_p, this nonlinear zonal advection involves the contribution from both mean and fluctuation, the latter of which is usually ignored in the previous works. The combined effect of this nonlinear advection, a mean easterly trade wind anomaly (Section 2.2 and 2.3) and effective stochastic noise was shown to facilitate the intermittent occurrence of the CP El Niño with realistic features [*Chen and Majda*, 2016].

2.2. Stochastic wind burst process

Stochastic parameterization of the wind activity is added to the model that represents several important ENSO triggers such as westerly wind bursts (WWBs), easterly wind bursts, as well as the convective envelope of the MJO. It also includes the recent multidecadal strengthening of the easterly trade wind anomaly. The wind bursts u_p reads:

$$u_p = a_p(\tau)s_p(x)\phi_0(y), \tag{5}$$

with amplitude $a_p(\tau)$ and fixed zonal spatial structure $s_p(x)$ shown in Figure 1. Here, $\phi_0(y)$ equals to the first parabolic cylinder function of the atmosphere (See Supporting Information). Both the wind burst perturbations [*Tziperman and Yu*, 2007] and the strengthening of the trade wind anomaly [*England et al.*, 2014; *Sohn et al.*, 2013] are localized over the western equatorial Pacific according to the observations and for simplicity they share the same zonal extent.

The evolution of wind burst amplitude a_p reads:

$$\frac{da_p}{d\tau} = -d_p(a_p \underline{-\hat{a}_p(T_W)}) + \sigma_p(T_W)\dot{W}(\tau), \tag{6}$$

where d_p is dissipation and $\dot{W}(\tau)$ is a white noise source, representing the intermittent nature of the wind bursts at interannual timescale. The amplitude of the wind burst noise source σ_p depends on $\mathrm{T_W}$, which is the average of SST anomalies in the western half of the equatorial Pacific ($0 \leq x \leq L_O/2$). The term $\hat{a}_p < 0$ represents the mean strengthening of the easterly trade wind anomaly. Corresponding to $\hat{a}_p < 0$, the direct response of the surface wind associated with the Walker circulation at the equatorial Pacific band is shown in Panel (c) of Figure 1, which is similar to the observed intensification of the Walker circulation in recent decades [*England et al.*, 2014; *Sohn et al.*, 2013].

2.3. A three-state Markov jump process

Due to the fact that the ENSO diversity is associated with the wind activity with distinct features [*Thual et al.*, 2016; *Chen and Majda*, 2016], a three-state Markov jump process [*Gardiner et al.*, 1985; *Lawler*, 2006; *Majda and Harlim*, 2012] is adopted to model the wind activity. Here, State 2 primarily corresponds to the traditional El Niño and State 1 to the CP El Niño while State 0 represents quiescent phases.

The following criteria are utilized in determining the parameters in (6) in each state. First, strong wind bursts play an important role in triggering the traditional El Niño [*Vecchi and Harrison*, 2000; *Tziperman and Yu*, 2007; *Hendon et al.*, 2007], which suggests a large noise amplitude σ_p in State 2. Secondly, the observational fact that an enhanced easterly trade wind accompanies with the CP El Niño since 1990s indicates a negative (easterly) mean $\hat{a}_p$ in State 1. To obtain the CP El Niño, the amplitude of $\hat{a}_p$ and the stochastic noise must be balanced [*Chen and Majda*, 2016]. This implies a relatively weak noise amplitude in State 1, which also agrees with observations [*Chen et al.*, 2015]. Finally, only weak wind activity is allowed in the quiescent state (State 0). Thus, the three states are given by

$$\text{State 2:} \qquad \sigma_{p2} = 2.7, \qquad d_{p2} = 3.4, \qquad \hat{a}_{p2} = -0.25, \tag{7}$$

$$\text{State 1:} \qquad \sigma_{p1} = 0.8, \qquad d_{p1} = 3.4, \qquad \hat{a}_{p1} = -0.25, \tag{8}$$

$$\text{State 0:} \qquad \sigma_{p0} = 0.5, \qquad d_{p0} = 3.4, \qquad \hat{a}_{p0} = 0, \tag{9}$$

respectively, where $d_p = 3.4$ represents a relaxation time around 10 days. Note that the same mean easterly wind anomaly as in State 1 is adopted in State 2, which allows occasional occurrences of the CP El Niño events in State 2 that improves the statistics of the model simulation. Since the amplitude of the stochastic noise dominates the mean easterly wind in State 2, this mean state has little impact on simulating the traditional El Niño events.

The local transition probability from State i to State j with $i \neq j$ for small $\Delta\tau$ is defined as follows

$$P(\sigma_p(\tau + \Delta\tau) = \sigma_{pj} | \sigma_p(\tau) = \sigma_{pi}) = \nu_{ij}\Delta\tau + o(\Delta\tau), \tag{10}$$

and the probability of staying in State i is given by

$$P(\sigma_p(\tau + \Delta\tau) = \sigma_{pi} | \sigma_p(\tau) = \sigma_{pi}) = 1 - \sum_{j\neq i} \nu_{ij}\Delta\tau + o(\Delta\tau). \tag{11}$$

Importantly, the transition rates ν_{ij} (with $i \neq j$) depend on $\mathrm{T_W}$. A transition ν_{ij} (with $i < j$) from a less active to a more active state is more likely when $\mathrm{T_W} \geq 0$ and vice versa. This allows for example a rapid shutdown of wind burst activity followed by extreme El Niño events, as in nature.

The transition rates are chosen in accordance with the observational record. For example, a higher transition probability from State 2 to State 0 is adopted compared with that to State 1, representing the situation that the traditional El Niño is usually followed by the La Niña rather than the CP El Niño. Likewise, starting from the quiescent phase, the model has a preference towards the occurrence of the CP El Niño rather than the eastern Pacific extreme El Niño. See Supporting Information for more details.

3. Results

Now we present the statistical diversity of ENSO produced by the coupled model. In order to compare the model simulations with the observational record, we define three indices from the model simulations: T-3, T-3.4 and T-4, which are the averaged SST over the regions of Nino 3 (150W-90W), Nino 3.4 (170W-120W) and Nino 4 (160E-150W), respectively.

Figure 2 shows the PDFs of T-4, T-3.4 and T-3 (Panel (a)-(c)) as well as the power spectrum of $\mathrm{T_E}$ (Panel (d)), which is the averaged SST over the eastern Pacific. These statistics are formed based on a 5000-year-long model simulation. The power spectrum of $\mathrm{T_E}$ peaks at the interannual band (3-7 years), which is consistent with nature [*Kleeman*, 2008]. The variance of all the three T indices almost perfectly match those of the three Nino indices (Panel (e)-(g); from NOAA). Particularly, the fact that the variance of SST in Nino 4 region being roughly half as much as that in the other two regions is captured by the coupled model. In addition, consistent with observations, the PDFs of T-4 and T-3 show negative and positive skewness, respectively. The presence of a fat tail together with the positive skewness in T-3 indicates the extreme El Niño events in the eastern Pacific as in nature [*Burgers and Stephenson*, 1999]. Note that, despite the correct skewed direction, the skewness of T-3 seems to be underestimated compared with Nino 3. Yet, the Nino indices are calculated based only on a 34-year-long monthly time-series (1982/01-2006/02), which may not be sufficient to form unbiased statistics. In fact, the single super El Niño event during 1997-1998 accounts for a large portion of the skewness in Nino 3. Therefore, the statistics of the model are qualitatively consistent with nature. The Supporting Information contains sensitivity tests, which show that the model statistics are fairly robust to parameter variations.

It is important to note that these non-Gaussian statistics indicate the significant role of both the nonlinear zonal advection and the state-dependent noise in the wind burst process, since otherwise the PDFs of T indices will all become Gaussian. In addition, in the absence of the CP El Niño [*Thual et al.*, 2016], the skewness of T-4 will become positive.

Figure 3 shows the time-series of three T indices, the stochastic wind amplitude a_p and the state transitions. Examples of the ENSO diversity are demonstrated in Figure 4 and 5. First, the coupled model succeeds in simulating traditional El Niño events in the eastern Pacific including both the quasi-regular moderate El Niño (e.g., $t = 181, 272, 292, 298$) and the super El Niño (e.g., $t = 199, 282$). These traditional El Niño events are typically followed by a reversal of conditions towards La Niña states ($t = 182, 200, 274, 284, 300$) with weaker strengths but longer durations (Column (d) in Figure 4 and 5). Particularly, the super El Niño appears every 15-25 years (See T-3 index), as in nature. These traditional El Niño events start with a realistic build-up of SST and thermocline depth anomalies in the western Pacific in the preceding year, which switches the system to the active state (State 2) and increases wind burst activity over the warm pool region. At the onset phase of these El Niño events, a strong series of WWBs (Column (f)) triggers enhanced thermocline depth and SST anomalies in the western Pacific, which then propagate eastward and intensify in the eastern Pacific at the peak of the El Niño events. However, there are many phases (e.g., $t = 186, 202, 296$) where wind burst activity builds up without triggering an El Niño event, implying that wind burst activity in the model is a necessary but non-sufficient condition to the El Niño development [*Hu et al.*, 2014; *Fedorov et al.*, 2015]. On the other hand, in the presence of the mean easterly wind anomaly and moderate wind activity, CP El Niño events are simulated by the coupled model (State 1), where the duration of these CP El Niño events varies from 1-2 years (e.g., $t = 175, 278, 290$) to 4-5 years (e.g., $t = 193$). Particularly, the period from $t = 193$ to $t = 201$ resembles the observed ENSO episode during 1990s, where a series of 5-year CP El Niño is followed by a super El Niño and then a La Niña.

Budget analysis indicates the distinct mechanisms of the two types of El Niño in the coupled model. The flux divergence $-\mu\partial_x(UT)$ appears to be the main contributor to the occurrence of the CP El Niño, where the westward zonal ocean current transports the anomalous warm water to the central Pacific region and leads to the eastern Pacific cooling with a shallow thermocline depth (See Column (h) and (i) in Figure 4 from $t = 193$ to $t = 197$). On the other hand, the dominant factor for the traditional El Niño is the thermocline feedback $c_1\eta H$, which is nearly proportional to the total SST tendency dT/dt (See Column (d) and (i) in Figure 4 around $t = 199$ and see Supporting Information for more details). All these findings in the model satisfy the analysis from the observational data [*Kao and Yu*, 2009; *Yu and Kao*, 2007; *Yeh et al.*, 2009, 2014; *Ren and Jin*, 2013].

Panel (j)-(l) in Figure 4 shows the anomalous Walker circulations at three different ENSO phases, which all agree with the observational record [*Kug et al.*, 2009]. Particularly, the surface wind $u + \hat{u}_p$ converges and forms the rising branch of the circulation in the central and eastern Pacific at the CP and traditional El Niño phases (t_1 and t_2), respectively. On the other hand, at the La Niña phase t_3, a descending branch of the anomalous Walker cell is found in the eastern Pacific, accompanying with the divergence of the surface wind.

4. Conclusions

A simple dynamical model is developed that automatically captures key features and the statistical diversity of ENSO. Systematic strategies are designed for incorporating several major causes of the ENSO diversity into a simple coupled ocean-atmosphere model that is otherwise deterministic, linear and stable. First, a stochastic parameterization of the wind bursts including both westerly and easterly wind is coupled to the ocean-atmosphere system, where the amplitude of the wind bursts depends on the SST in the western Pacific warm pool. Secondly, a simple nonlinear zonal advection and a mean easterly trade wind anomaly are incorporated into the coupled system that enables anomalous warm sea surface temperature in the central Pacific. Finally, a three-state Markov jump process is developed to drive the stochastic wind activity, which allows the occurrence of different types of ENSO.

The statistics produced by the coupled model resemble those of nature. The power spectrum of T_E peaks at the interannual band. The variance of the three T indices almost perfectly match those in the observational record of Nino 3, 3.4 and 4 indices and the directions of the skewness of the T and the Nino indices are the same in all three regions. Importantly, the fat tail together with the positive skewness in the PDF of T-3 index implies the intermittent occurrence of the extreme El Niño events.

The coupled model succeeds in simulating both the CP and the traditional El Niño events, including quasi-regular moderate El Niño and super El Niño, as well as the La Niña with realistic features. Particularly, the model is able to reproduce the observed ENSO episode with diversity in 1990s. In addition, the anomalous Walker circulation at different ENSO phases all resembles nature.

Acknowledgments. The research of A.J.M. is partially supported by the Office of Naval Research Grant ONR MURI N00014-16-1-2161 and the New York University Abu Dhabi Research Institute. N.C. is supported as a postdoctoral fellow through A.J.M's ONR MURI Grant.

References

Ashok, K., S. K. Behera, S. A. Rao, H. Weng, and T. Yamagata (2007), El Nino Modoki and its possible teleconnections., *J. Geophys. Res*, *112*.

Ault, T., C. Deser, M. Newman, and J. Emile-Geay (2013), Characterizing decadal to centennial variability in the equatorial Pacific during the last millennium, *Geophysical Research Letters*, *40*(13), 3450–3456.

Burgers, G., and D. B. Stephenson (1999), The "normality" of El Niño, *Geophys. Res. Lett*, *26*(8), 1027–1039.

Capotondi, A., A. T. Wittenberg, M. Newman, E. Di Lorenzo, J.-Y. Yu, P. Braconnot, J. Cole, B. Dewitte, B. Giese, E. Guilyardi, et al. (2015), Understanding ENSO diversity, *Bulletin of the American Meteorological Society*, *96*(6), 921–938.

Chen, D., T. Lian, C. Fu, M. A. Cane, Y. Tang, R. Murtugudde, X. Song, Q. Wu, and L. Zhou (2015), Strong influence of westerly wind bursts on El Niño diversity, *Nature Geoscience*, *8*(5), 339–345.

Chen, N., and A. J. Majda (2016), Simple dynamical models capturing the key features of the central Pacific El Niño, *Proceedings of the National Academy of Sciences*, in press and to appear on Oct 3.

Choi, J.-W., I.-G. Kim, J.-Y. Kim, and C.-H. Park (2016), The recent strengthening of Walker circulation, *SOLA*, *12*(0), 96–99.

Clarke, A. J. (2008), *An Introduction to the Dynamics of El Nino & the Southern Oscillation*, Academic press.

Dewitte, B., S.-W. Yeh, and S. Thual (2013), Reinterpreting the thermocline feedback in the western-central equatorial Pacific and its relationship with the ENSO modulation, *Climate dynamics*, *41*(3-4), 819–830.

England, M. H., S. McGregor, P. Spence, G. A. Meehl, A. Timmermann, W. Cai, A. S. Gupta, M. J. McPhaden, A. Purich, and A. Santoso (2014), Recent intensification of wind-driven circulation in the Pacific and the ongoing warming hiatus, *Nature Climate Change*, *4*(3), 222–227.

Fedorov, A. V., S. Hu, M. Lengaigne, and E. Guilyardi (2015), The impact of westerly wind bursts and ocean initial state on the development, and diversity of El Niño events, *Climate Dynamics*, *44*(5-6), 1381–1401.

Gardiner, C. W., et al. (1985), *Handbook of Stochastic Methods*, vol. 3, Springer Berlin.

Guilyardi, E. (2006), El Nino–mean state–seasonal cycle interactions in a multi-model ensemble, *Climate Dynamics*, *26*(4), 329–348.

Ham, Y.-G., and J.-S. Kug (2012), How well do current climate models simulate two types of El Nino?, *Climate dynamics*, *39*(1-2), 383–398.

Hendon, H. H., M. C. Wheeler, and C. Zhang (2007), Seasonal dependence of the MJO-ENSO relationship, *Journal of Climate*, *20*(3), 531–543.

Hu, S., A. V. Fedorov, M. Lengaigne, and E. Guilyardi (2014), The impact of westerly wind bursts on the diversity and predictability of El Niño events: an ocean energetics perspective, *Geophysical Research Letters*, *41*(13), 4654–4663.

Jin, F.-F., and S.-I. An (1999), Thermocline and zonal advective feedbacks within the equatorial ocean recharge oscillator model for ENSO, *Geophysical research letters*, *26*(19), 2989–2992.

Kao, H.-Y., and J.-Y. Yu (2009), Contrasting eastern-Pacific and central-Pacific types of ENSO, *Journal of Climate*, *22*(3), 615–632.

Kim, S. T., and J.-Y. Yu (2012), The two types of ENSO in CMIP5 models, *Geophysical Research Letters*, *39*(11).

Kleeman, R. (2008), Stochastic theories for the irregularity of ENSO, *Philosophical Transactions of the Royal Society of London A: Mathematical, Physical and Engineering Sciences*, *366*(1875), 2509–2524.

Kug, J.-S., F.-F. Jin, and S.-I. An (2009), Two types of El Niño events: cold tongue El Niño and warm pool El Niño, *Journal of Climate*, *22*(6), 1499–1515.

Kug, J.-S., J. Choi, S.-I. An, F.-F. Jin, and A. T. Wittenberg (2010), Warm pool and cold tongue El Niño events as simulated by the GFDL 2.1 coupled GCM, *Journal of Climate*, *23*(5), 1226–1239.

Kug, J.-S., Y.-G. Ham, J.-Y. Lee, and F.-F. Jin (2012), Improved simulation of two types of El Niño in CMIP5 models, *Environmental Research Letters*, *7*(3), 034,002.

Larkin, N. K., and D. Harrison (2005), On the definition of El Niño and associated seasonal average US weather anomalies, *Geophysical Research Letters*, *32*(13).

Lawler, G. F. (2006), *Introduction to Stochastic Processes*, CRC Press.

Lee, T., and M. J. McPhaden (2010), Increasing intensity of El Niño in the central-equatorial Pacific, *Geophysical Research Letters*, *37*(14).

L'Heureux, M. L., S. Lee, and B. Lyon (2013), Recent multidecadal strengthening of the Walker circulation across the tropical Pacific, *Nature Climate Change*, *3*(6), 571–576.

Majda, A. (2003), *Introduction to PDEs and Waves for the Atmosphere and Ocean*, vol. 9, American Mathematical Soc.

Majda, A. J., and J. Harlim (2012), *Filtering Complex Turbulent Systems*, Cambridge University Press.

Majda, A. J., and R. Klein (2003), Systematic multiscale models for the tropics, *Journal of the Atmospheric Sciences*, *60*(2), 393–408.

Majda, A. J., and S. N. Stechmann (2009), The skeleton of tropical intraseasonal oscillations, *Proceedings of the National Academy of Sciences*, *106*(21), 8417–8422.

Majda, A. J., and S. N. Stechmann (2011), Nonlinear dynamics and regional variations in the MJO skeleton, *Journal of the Atmospheric Sciences*, *68*(12), 3053–3071.

McGregor, S., A. Timmermann, M. F. Stuecker, M. H. England, M. Merrifield, F.-F. Jin, and Y. Chikamoto (2014), Recent Walker circulation strengthening and Pacific cooling amplified by Atlantic warming, *Nature Climate Change*, *4*(10), 888–892.

Merrifield, M. A., and M. E. Maltrud (2011), Regional sea level trends due to a Pacific trade wind intensification, *Geophysical Research Letters*, *38*(21).

Ren, H.-L., and F.-F. Jin (2013), Recharge oscillator mechanisms in two types of ENSO, *Journal of Climate*, *26*(17), 6506–6523.

Sohn, B., S.-W. Yeh, J. Schmetz, and H.-J. Song (2013), Observational evidences of Walker circulation change over the last 30 years contrasting with GCM results, *Climate Dynamics*, *40*(7-8), 1721–1732.

Stechmann, S. N., and A. J. Majda (2015), Identifying the skeleton of the Madden–Julian oscillation in observational data, *Monthly Weather Review*, *143*(1), 395–416.

Stechmann, S. N., and H. R. Ogrosky (2014), The Walker circulation, diabatic heating, and outgoing longwave radiation, *Geophysical Research Letters*, *41*(24), 9097–9105.

Su, J., T. Li, and R. Zhang (2014), The initiation and developing mechanisms of central Pacific El Niños, *Journal of Climate*, *27*(12), 4473–4485.

Thual, S., O. Thual, and B. Dewitte (2013), Absolute or convective instability in the equatorial Pacific and implications for ENSO, *Quarterly Journal of the Royal Meteorological Society*, *139*(672), 600–606.

Thual, S., A. J. Majda, N. Chen, and S. N. Stechmann (2016), Simple stochastic model for El Niño with westerly wind bursts, *Proceedings of the National Academy of Sciences*, p. 201612002.

Tziperman, E., and L. Yu (2007), Quantifying the dependence of westerly wind bursts on the large-scale tropical Pacific SST, *Journal of climate*, *20*(12), 2760–2768.

Vecchi, G. A., and D. Harrison (2000), Tropical Pacific sea surface temperature anomalies, El Nino, and equatorial westerly wind events, *Journal of climate*, *13*(11), 1814–1830.

Weng, H., S. K. Behera, and T. Yamagata (2009), Anomalous winter climate conditions in the Pacific rim during recent El Niño Modoki and El Niño events, *Climate Dynamics*, *32*(5), 663–674.

Wittenberg, A. T. (2009), Are historical records sufficient to constrain ENSO simulations?, *Geophysical Research Letters*, *36*(12).

Yeh, S.-W., J.-S. Kug, B. Dewitte, M.-H. Kwon, B. P. Kirtman, and F.-F. Jin (2009), El Niño in a changing climate, *Nature*, *461*(7263), 511–514.

Yeh, S.-W., J.-S. Kug, and S.-I. An (2014), Recent progress on two types of El Niño: observations, dynamics, and future changes, *Asia-Pacific Journal of Atmospheric Sciences*, *50*(1), 69–81.

Yu, J.-Y., and H.-Y. Kao (2007), Decadal changes of ENSO persistence barrier in SST and ocean heat content indices: 1958–2001, *Journal of Geophysical Research: Atmospheres*, *112*(D13).

Yu, J.-Y., and S. T. Kim (2010), Identification of central-Pacific and eastern-Pacific types of ENSO in CMIP3 models, *Geophysical Research Letters*, *37*(15).

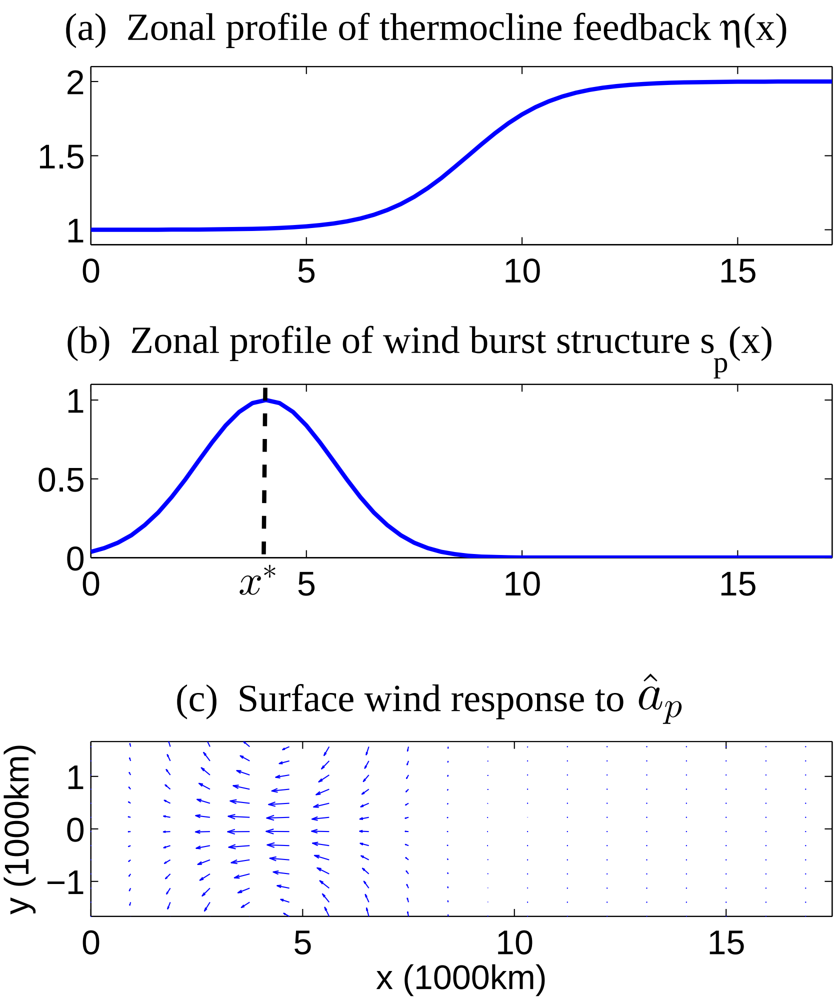

Figure 1. Profiles of (a) the thermocline coefficient $\eta(x)$, (b) the zonal structure of the wind burst $s_p(x)$ with its peak at x^*, and (c) the surface wind response in equatorial Pacific band (from 15^oS to 15^oN) to a mean easterly trade wind anomaly $\hat{a}_p$.

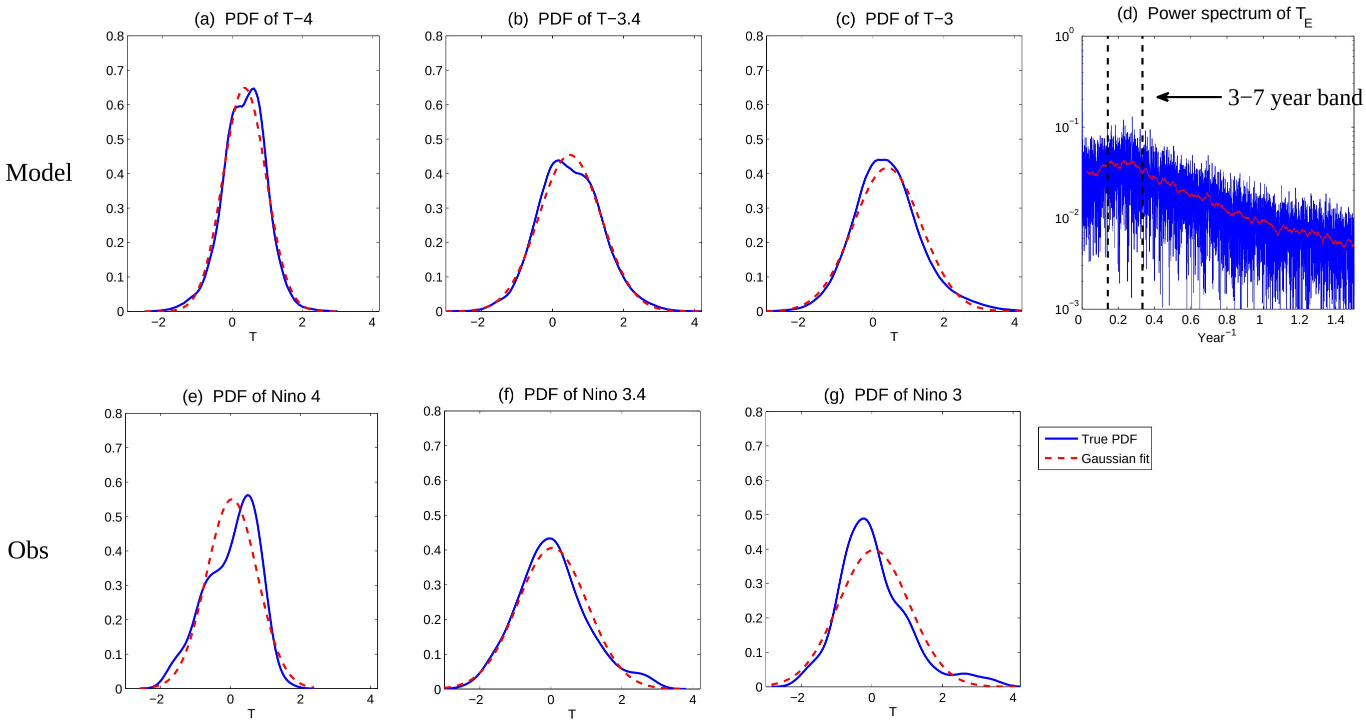

Figure 2. PDFs of T-3, T-3.4 and T-4 from the coupled model (Panel (a)-(c)) and those of Nino 3, 3.4 and 4 from NOAA observational record (1982/01-2016/02; Panel (e)-(g)). Panel (d) shows the power spectrum of T_E, where the red curve is the running average. The model statistics are computed based on a 5000-year-long simulation.

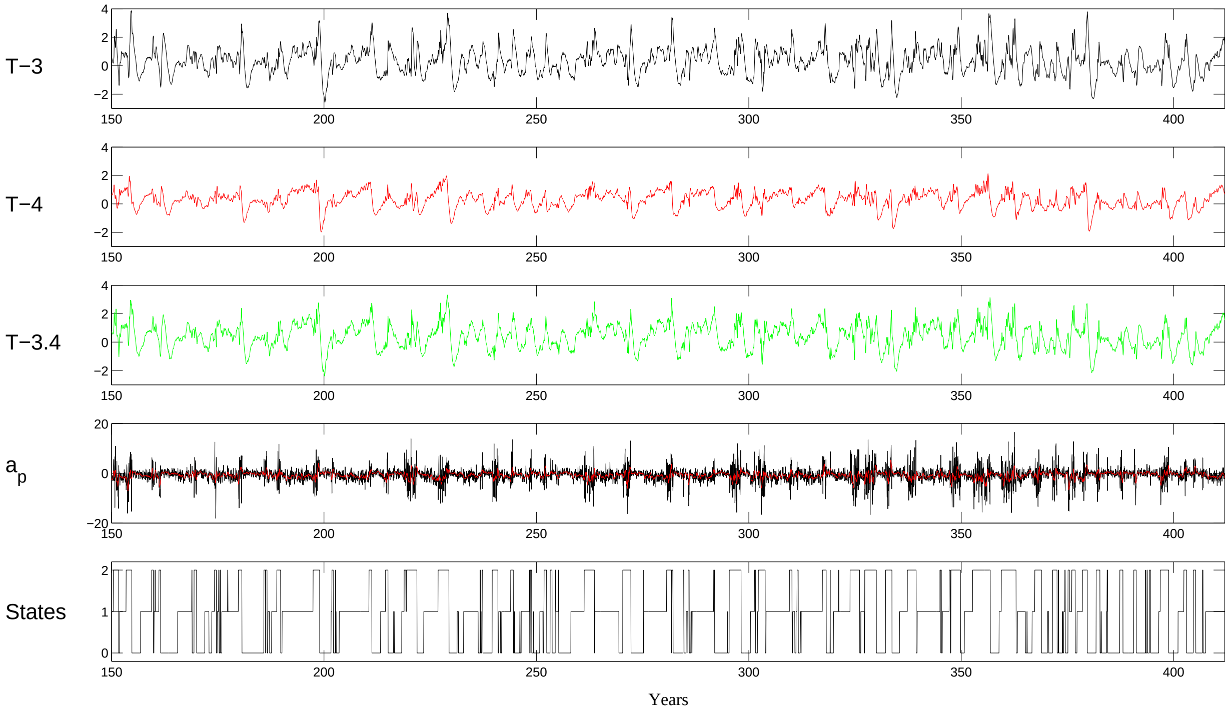

Figure 3. A sample period of time-series T-3, T-4, T-3.4, the stochastic wind activity amplitude a_p and the states in the Markov process.

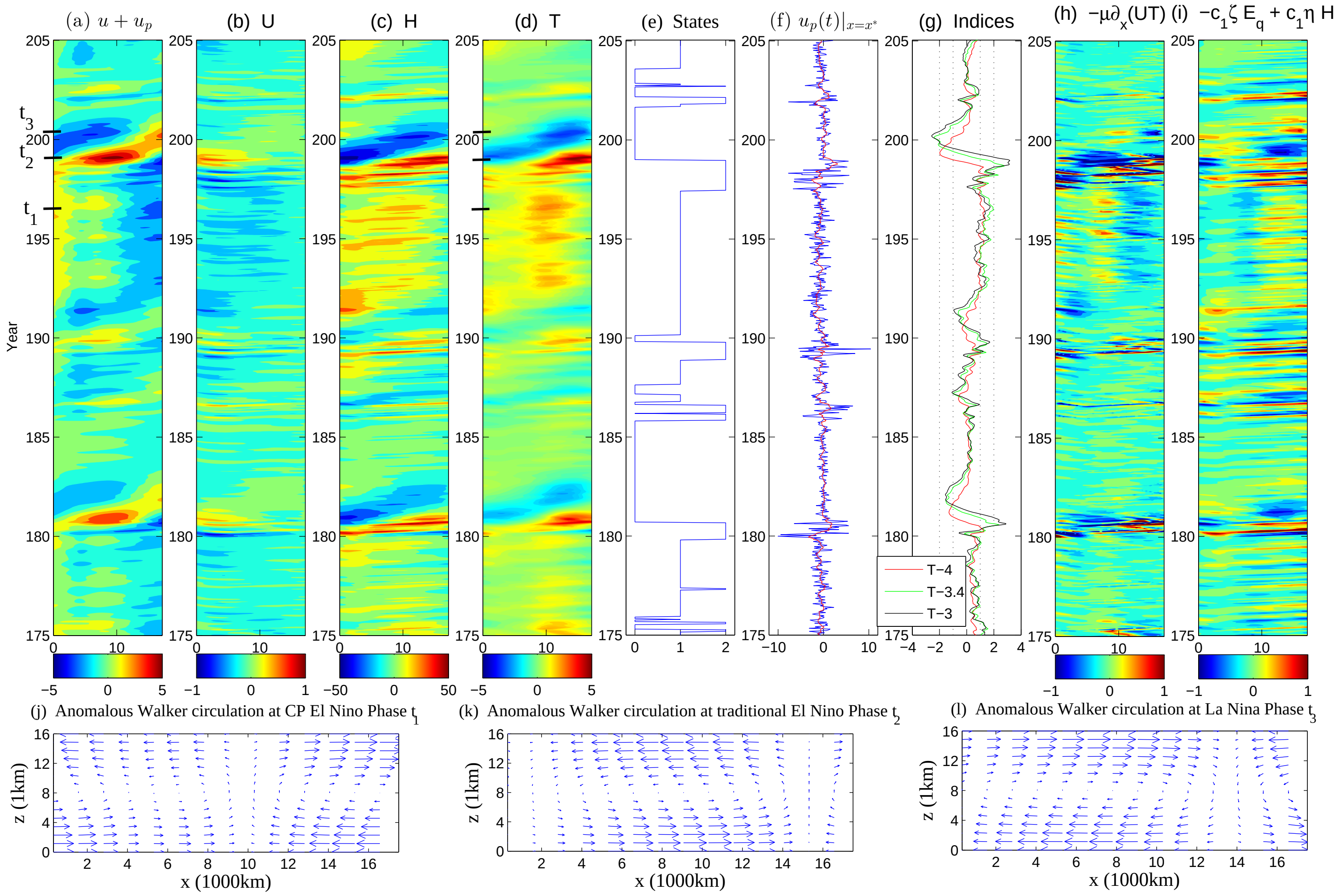

Figure 4. Period from $t = 175$ to $t = 205$ in Figure 3. Column (a)-(d): Hovmoller diagram of atmospheric wind $u + u_p$, ocean zonal current U, thermocline depth H and SST anomaly T. Column (e)-(g): Transitions of the states, stochastic wind u_p at the longitude $x = x^*$ with its maximum value, and T indices. Column (h)-(i): budget of flux divergence $-\partial_x(UT)$ and the summation of latent heating $-c_1\zeta E_q$ and thermocline feedback $c_1\eta H$. Column (j)-(l): anomalous Walker circulation at three different ENSO phases in Column (a).

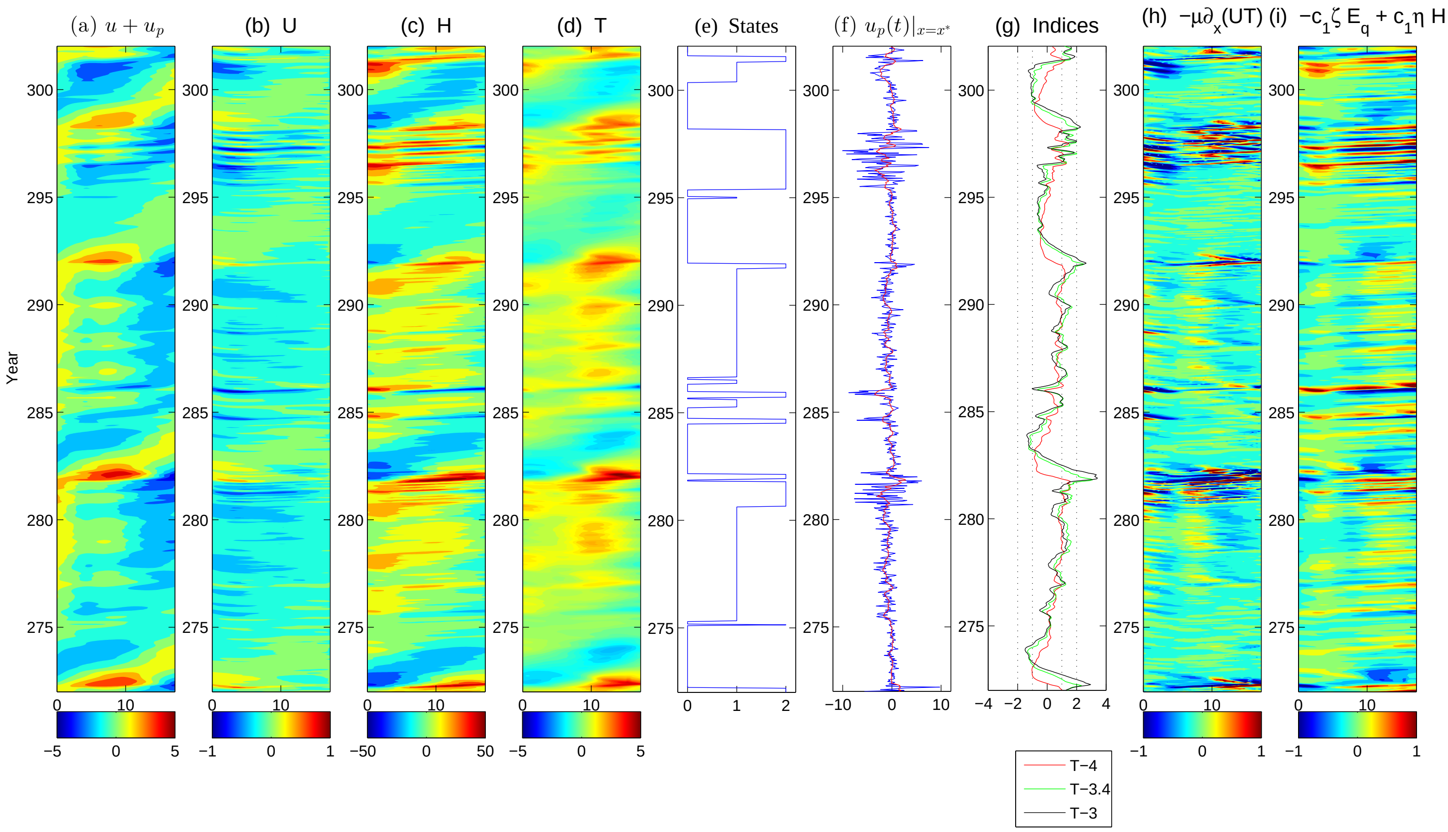

Figure 5. Same as Column (a)-(i) in Figure 4 but from $t = 272$ to $t = 302$.